Molecular Simulation
Vol. 00, No. 0, 2012, 1–6

Taylor & Francis
Taylor & Francis Group

Effect of thiol-functionalised silica on *cis*platin adsorption

Andres Díaz Compañy[a], Alfredo Juan[a], Graciela Brizuela[a] and Sandra Simonetti[a,b]*

[a]*Departamento de Física, Universidad Nacional del Sur, Av. Alem 1253, 8000 Bahía Blanca, Argentine;* [b]*Departamentos de Ciencias Básicas e Ingeniería Mecánica, Universidad Tecnológica Nacional, 11 de Abril 461, 8000 Bahía Blanca, Argentine*

(*Received 5 March 2012; final version received 29 April 2012*)

This study contributes to the investigation related to guest–host interactions between the chemotherapeutic agent *cis*platin and a functionalised silica matrix in order to improve and find new materials such as drug carriers. The adsorption of *cis*platin and its complexes, *cis*-$[PtCl(NH_3)_2]^+$ and *cis*-$[Pt(NH_3)_2]^{2+}$, on a SH-functionalised $SiO_2(111)$ surface has been studied by the atom superposition and electron delocalisation method. The adiabatic energy curves for the adsorption of the drug and its products on the delivery system were considered. The electronic structure and bonding analysis were also performed. The molecule and their complex are adsorbed on the functionalised surface resulting in a major absorption of the *cis*-$[Pt(NH_3)_2]^{2+}$ complex. The molecule–surface interactions are formed via —SH group. The molecule/complexes SH electron-donating effect plays an important role in the catalytic reaction. The more important drug–carrier interactions occur through the Cl—H bond for the adsorption of *cis*-$[PtCl_2(NH_3)_2]$ and *cis*-$[PtCl(NH_3)_2]^+$, and through the Pt—S and Pt—H interactions for *cis*-$[Pt(NH_3)_2]^{2+}$ adsorption. When the new interactions are formed, the functionalised carrier maintains their matrix properties while the molecule is the most affected after adsorption. The Pt atomic orbitals present the most important changes during adsorption.

Keywords: *cis*platin; silica; adsorption; functionalisation; drug delivery

1. Introduction

The recent emergence of the periodic mesoporous materials becomes an active area of research because of their exciting potential applications in catalysis, separation, drug delivery, nanocomposites and confinement of electronic materials. Each mesoporous material has its own typical features that differ from those of others, such as mesostructure, pore size, surface area and pore volume. In the practical reaction, their characteristics could have a great effect on the results of catalytic behaviour, such as activity, selectivity and product yield.

Functional groups can increase the adsorption performance of mesoporous silica [1]. Different types of immobilisation of metal complexes were performed through a coordination bond with functional groups on the mesoporous supports. There have been dramatic developments in the studies on surface functionalisation of mesoporous materials [2–5]. For the functionalisation, aliphatic hydrocarbon [6], phenyl [7], amine [8] and vinyl, benzyl, phenyl, cyano, mercapto, aminopropyl or dihydroimidazole [9] ligands have been mainly studied as surface functional groups.

Functionalised mesoporous materials for adsorption and release of different drug molecules have been studied by Wang et al. The different functional groups introduced into the materials dictated their adsorption capacity and release properties. While mercaptopropyl- and vinyl-functionalised samples showed high adsorption capacity for rhodamine 6G, amine-functionalised samples exhibited higher adsorption capacity for ibuprofen [10].

Luminescent organic–inorganic hybrids of functionalised mesoporous silica have been investigated by Li et al. using thio-salicylidene schiff base. The synthesis of bis(salicylidene)-thiocarbohydrazide (BSTC-SBA-15) provides a convenient approach of tailoring the surface properties of mesoporous silicates by organic functionalisation, and all the resulting materials retain the ordered mesoporous structures [11].

A recyclable thiol-functionalised mesoporous silica for detection and removal of Cu(II) ions has been studied by Li et al. The adsorption capacity of the recycled silicas remains the same as that of the freshly prepared, which makes them promising adsorbents for wastewater cleanup [12].

Sulphonic-functionalised mesoporous materials received exceptional attention because of their numerous practical applications in heterogeneous acid catalysis, toxic mercury ion trapping, biomolecule immobilisation and as a support material for metallic nanoparticles [13].

Many of the current chemotherapeutic drugs cause severe toxicity to the body, such as hair loss and nausea, when administered at high systemic doses. The optimisation of the dosing through delivery systems can potentially minimise the adverse effects while maintaining

*Corresponding author. Email: ssimonet@uns.edu.ar

ISSN 0892-7022 print/ISSN 1029-0435 online

http://dx.doi.org/10.1080/08927022.2012.690875
http://www.tandfonline.com

efficacy. The objective of this project is to study the adsorption properties of thiol-functionalised porous silica as vehicles for the local and sustained delivery of the chemotherapeutic agent: *cis*platin. *Cis*platin (*cis*-diamine-dichloroplatinum [II]) is a coordination compound used in the treatment of several solid tumours [14,15]. It is a well-known square planar complex with chemical formula *cis*-$[Pt(NH_3)_2Cl_2]$, first described by Michel Peyrone in 1844. The structure was elucidated by Alfred Werner nearly 50 years later in 1893. Aiming to predict potentially active species in the mode of action of the anticancer drug *cis*platin, the study focused on the hydrolysis of one or both platinum-chloro bonds of the drug [16,17] also on the functionalised matrix. The energy curves for the adsorption of *cis*platin and its complexes on the thiol-functionalised silica are calculated by the atom superposition and electron delocalisation (ASED) method. The electronic structure and the chemical bonding after adsorption are also addressed.

2. Computational method

Our calculations were performed using the ASED method [18–21]. This method is a modification of the extended Hückel molecular orbital method implemented with the yet another extended Hückel molecular orbital package program [22]. The ASED theory is based on a physical model of molecular and solid electronic charge density distribution functions [21–24].

The adiabatic total energy values were computed as the difference between the electronic energy (E) of the system when the drug is at finite distance on the functionalised surface (carrier) and the same energy when it is far away from the surface:

$$\Delta E_{\mathrm{Abs,\,total}} = E\,(\mathrm{carrier} + \mathrm{drug}) - E\,(\mathrm{carrier}) - E\,(\mathrm{drug}).$$

The repulsive energy was computed taking into account all atom–atom interactions.

To understand the drug–carrier interactions, we used the concept of density of states (DOS) and crystal orbital overlap population (COOP) curves. The DOS curve is a plot of the number of orbitals per unit volume per unit energy. The COOP curve is a plot of the overlap population (OP)-weighted DOS versus energy. The integration of the COOP curve up to the Fermi level (E_f) gives the total OP of the bond specified, and it is a measure of the bond strength.

3. The drug–carrier system

A silicon dioxide-hydrated matrix was performed to simulate the solid carrier according De Boer et al.'s [25] model. The original cluster has 209 atoms (27 hydrogens, 128 oxygens and 54 silicons). The cluster was functionalised by introducing SH silane groups stream replacing 50% of the hydroxyl groups of the surface. The starting point for the calculation is the *cis*platin structure taken from the experimental data [26,27]. During the calculations, the structures of both molecule and substrate were optimised at steps of 0.02 Å and convergence in energy by 0.01 eV. Different molecule/fragments orientations and adsorption sites on the functionalised silica surface were taken in order to obtain the optimum adsorption geometry and the preferential adsorption site. The most favourable corresponds to the vertical adsorption of the molecule, and its fragments in a way that the Cl atoms are closer to the SH groups of the silica surface. Figure 1 shows a schematic representation of *cis*platin/complexes silica adsorption geometry. We have computed the adiabatic energy of the system by absorbing the drug on the SiO_2(111)-functionalised surface. We have obtained the energy curves, initially for the *cis*platin molecule and then, considering the removal of one and the two chloro atoms of the molecule, in order to analyse the hydrolysis products adsorption. Then, we have studied the major electronic interactions between the drug/fragments and the thiol-functionalised silica surface.

4. Results and discussion

The adsorption energies for *cis*platin and its complexes are shown in Figure 2. For *cis*-$[PtCl_2(NH_3)_2]$ adsorption, the system becomes more stable considering the SH—Cl distances above 3.2 Å, showing a weak molecule–surface absorption (see Figure 1(a)). We can see the inexistence of a minimum energy position. For the $[PtCl(NH_3)_2]^+$ complex, we can see in Figure 1(b) that the system is more stable when this complex is from 2.6 Å on the surface and again the adsorption is weak without a minimum energy location for the complex. In opposition, for the *cis*-$[Pt(NH_3)_2]^{2+}$ adsorption, the system is most stable when the complex is 0.2 Å to the surface and now the existence of a minimum energy position for the complex is evident (see Figure 1(c)). Considering the hoped balance between the *cis*platin and its products [6–8] and analysing the energy curves (Figure 1), we can conclude that the molecule and their complex can adsorb on the functionalised surface resulting in a major absorption of the *cis*-$[Pt(NH_3)_2]^{2+}$ complex.

Figure 2(a) shows the DOS curve for the *cis*-$[PtCl_2(NH_3)_2]$–silica system. If we compare the corresponding isolated functionalised silica with Figure 2(b), the changes are small because the presence of molecule is almost negligible. The contributions to the DOS of the *cis*platin orbitals are evident if those are magnified by a factor of 100 in Figure 2(c). The horizontal sticks display the energy of the molecular orbitals in the isolated *cis*platin. We can see the bands' dispersion due to the interaction with the functionalised silica surface. After adsorption, the bands are spread over and a portion of its DOS is pushed above the

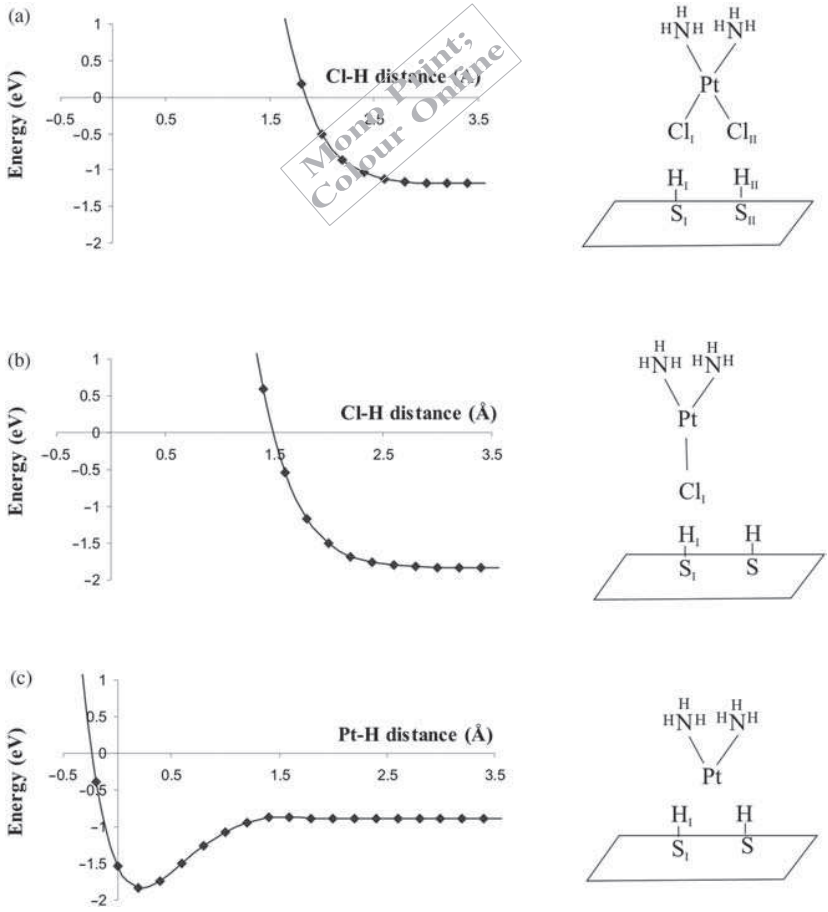

Figure 1. Adiabatic energy curves for the (a) *cis*platin/silica–SH system, (b) *cis*-$[PtCl(NH_3)_2]^+$/silica–SH system and (c) *cis*-$[Pt(NH_3)_2]^{2+}$/silica–SH system. The schematic view of the adsorption geometries is indicated.

Fermi level. The value of the Fermi energy (E_f) of the *cis*-$[PtCl_2(NH_3)_2]$–silica system is -11.56 eV and it changes slightly with respect to the isolated silica ($E_f = -12.52$ eV).

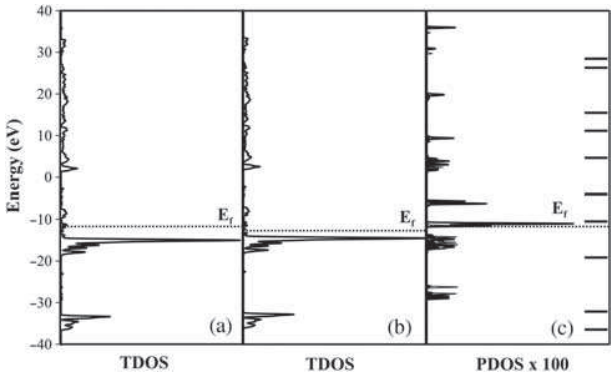

Figure 2. (a) Total DOS for the *cis*platin/silica–SH system, (b) total DOS for the isolated silica–SH system and (c) projected DOS for the *cis*platin molecule adsorbed on the silica–SH surface. The horizontal solid lines indicate the orbital positions in the isolated *cis*platin molecule.

The states below the Fermi level mainly correspond to the silicon conduction band.

According to the most favourable adsorption energy ranges for the molecule and their complexes, we have selected one configuration of each sub-system in order to perform the electronic structure analysis and bonding considerations.

For *cis*-$[PtCl_2(NH_3)_2]$–silica system, we have selected the geometry corresponding to the molecule–surface distance (Cl—H distance) of 3.2 Å. For this configuration, each Cl atoms to the *cis*platin have very small interactions with the H atoms of two nearest-neighbour SH groups of the functionalised surface. The existence of these bonds is confirmed by the bond population, the Cl—H OPs are both 0.0006. The COOP curve is shown in Figure 3(a). This curve presents bonding and anti-bonding peaks below the Fermi energy level (E_f). The integration up to the Fermi level gives the total OP for the Cl—H bonding. On the other hand, the Cl—Si interactions are almost negligible and there is no evidence for Cl—S and Cl—O interactions.

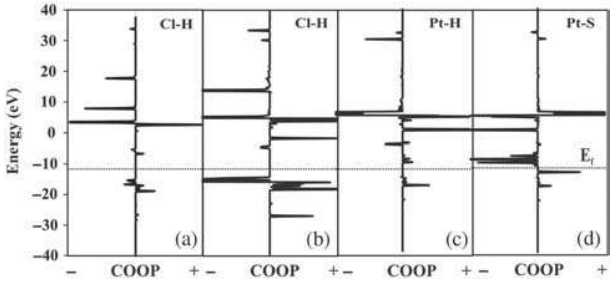

Figure 3. COOP curves for (a) the Cl—H interaction in the *cis*platin/silica–SH system, (b) the Cl—H interaction in the *cis*-$[PtCl(NH_3)_2]^+$/silica–SH system, (c) Pt—H and (d) Pt—S interactions in the *cis*-$[Pt(NH3)2]^{2+}$/silica–SH system.

For *cis*-$[PtCl(NH_3)_2]^+$–silica system, we have selected the geometry corresponding to the complex located at 2.6 Å to the surface. For this configuration, the Cl atom has an interaction with an H atom of a SH group of the surface. The Cl—H bond population is 0.0032. The interaction is small but bigger than the Cl—H interaction as described previously; the COOP curve is shown in Figure 3(b). A very little Cl—Si interaction is observed and no evidence for Cl—S and Cl—O interactions is noticed.

For *cis*-$[Pt(NH_3)_2]^{2+}$–silica system, we have considered the geometry corresponding to the complex located at the minimum energy position of 0.2 Å to the surface. When the two chloro atoms are removed, the most favourable interactions occur between the Pt and both S and H atoms of neigbouring SH groups. The Pt—S and Pt—H OP values are 0.0026 and 0.0017, respectively; Figure 3(c) and (d) shows the COOP curves that mainly correspond to a bonding interactions. On the other hand, the Pt—Si interaction is not evident.

The adsorption of the drug is possible because it produced a rearrangement of the electronic densities of the solid-functionalised surface and the *cis*platin atomic orbitals. The major changes are summarised in Table 1.

For *cis*-$[PtCl_2(NH_3)_2]$–silica system, the OPs of the S and H atoms of the surface modified less than 0.02%, the major changes are observed in S p_x and H s orbitals; while the Cl s and Cl p orbitals of the molecule decrease 0.4% and 20%, respectively, the most important changes are presented in Cl p_y and Cl p_z orbitals. The s, p and d OPs of the Pt atom are decreased by 32%, 5%, and 85%, respectively; the bigger changes are observed in Pt s, $d_z^2 - d_y^2$, d_{xy} and d_{yz} orbitals. Then, for *cis*-$[PtCl_2(NH_3)_2]$–silica interaction, the most affected are the Cl p, Pt s and Pt d OPs.

For *cis*-$[PtCl(NH_3)_2]^+$–silica system, the H s population of SH superficial group are decreased by 0.3%, whereas the corresponding s and p OPs of the S atom are increased by less than 0.2%. The s and p OPs of the Cl atom are decreased by 0.3% and 6%, respectively, the major change is present in Cl p_y orbital; whereas the s, p, and d OPs of the Pt atom are decreased by 32%, 26% and 88%, respectively, the bigger changes are observed in Pt d_z^2 and d_{yz} orbitals. Therefore, the Pt atomic orbitals of the *cis*-$[PtCl(NH_3)_2]^+$ complex are the most affected after adsorption.

Table 1. Orbital occupations, net charges and OP for the atoms which participate in the interactions.

	Orbital occupation				
	s	p	D	Bond	OP
H_I	0.8237[a]				0.0006[a]
	0.8215[b]			Cl—H	0.0032[b]
	0.8236[c]				–
	0.8239[d]				–
H_{II}	0.8237[a]				–
	0.8239[b]			Pt—H	–
	0.8236[c]				0.0017[c]
	0.8239[d]				–
S_I	1.3305[a]	4.6416[a]			–
	1.3326[b]	4.6450[b]		Pt—S	–
	1.3301[c]	4.6382[c]			0.0026[c]
	1.3302[d]	4.6411[d]			–
S_{II}	1.3305[a]	4.6416[a]			0.7190[a]
	1.3302[b]	4.6411[b]		Pt—Cl	0.9155[b]
	1.3301[c]	4.6383[c]			–
	1.3302[d]	4.6411[d]			0.5345[d]
Cl_I	1.8548[a]	4.4125[a]			0.7317[a]
	1.8562[b]	5.1891[b]		S—H	0.7320[b]
	–	–			0.7310[c]
	1.8613[d]	5.5367[d]			0.7320[d]
Cl_{II}	1.8536[a]	4.4091[a]			
	–	–			
	–	–			
	1.8612[d]	5.5369[d]			
Pt	0.4487[a]	0.8501[a]	1.2926[a]		
	0.4451[b]	0.6617[b]	1.0105[b]		
	0.3389[c]	0.2679[c]	0.6277[c]		
	0.6591[d]	0.8921[d]	8.5948[d]		

[a] *Cis*-$[PtCl_2(NH_3)_2]$/silica–SH system. [b] *Cis*-$[PtCl(NH_3)_2]^+$/silica–SH system. [c] *Cis*-$[Pt(NH_3)_2]^{2+}$/silica–SH system. [d] Isolated silica–SH or isolated *cis*platin.

For *cis*-$[Pt(NH_3)_2]^{2+}$–silica system, the H s population of SH group is decreased by 0.03%, whereas the corresponding s and p OPs of the S atom are decreased in a lesser amount. The s, p and d OPs of the Pt atom are decreased by 48%, 67%, and 93%, respectively, the major changes are observed in Pt p_y, p_z, $d_z^2 - d_y^2$, d_{xy} and d_{yz} orbitals. Consequently, for *cis*-$[Pt(NH_3)_2]^{2+}$ adsorption, the major changes are produced in Pt OPs.

In general, it can be observed that after adsorption the molecule presents bigger changes than the functionalised surface.

The electron exchange helps to form the absorbate–substrate interactions. For *cis*-$[PtCl_2(NH_3)_2]$–silica system, it is observed that an electron transfer to the Pt, Cl, and H atoms to the S atom. For *cis*-$[PtCl(NH_3)_2]^+$–silica system, it is observed that an electron transfer to the Pt and H atoms to the Cl and S atoms; while for *cis*-$[Pt(NH_3)_2]^{2+}$–silica system, it is observed that an electron transfer to the Pt and H atoms to the S atoms.

In general, when the new interactions are formed, the strength of the SH bond practically is not affected after adsorption (less than 0.5%, see Table 1). In opposite, in the molecule, the Cl—Pt interaction is affected after adsorption. The C—Pt OP in the isolated molecule is 0.5345 and increases to 0.7190 (26%) and 0.9155 (42%) during the adsorption of *cis*-$[PtCl_2(NH_3)_2]$ and *cis*-$[PtCl(NH_3)_2]^+$, respectively. We can conclude that the carrier matrix maintains their properties after adsorption, and the Cl—Pt bond in the molecule/*cis*-$[PtCl(NH_3)_2]^+$ complex is strengthened after adsorption.

5. Conclusions

This paper contributes to the investigation in relation to guest–host interactions between *cis*platin and a SH-functionalised silica matrix in order to improve and find new materials such as drug carriers.

The adsorption of *cis*platin on a SH-functionalised SiO_2(111) surface was investigated by tight binding calculation. We were able to evaluate the simultaneous manifestation of true confinement and surface effects in this silica host for a drug. Starting from the optimisation of the adsorption geometries for the drug and its complexes, we could reproduce the main characteristics of the adsorption process. We have also analysed the nature of the drug–carrier bonding and the changes observed in the electronic structure upon adsorption.

The silica–SH carrier showed catalytic properties. Except those molecular orbitals lying much lower in energy, the rest are modified showing the molecule–surface interaction. From the energy plots, the molecule and their complex are adsorbed on the functionalised surface resulting in a major absorption of the therapeutic *cis*-$[Pt(NH_3)_2]^{2+}$ complex.

We have computed the new bondings by the OP and COOP curves. The new interactions are formed via the SH groups. It was found that the molecule/complex SH electron-donating effect plays an important role in the catalytic reaction. The drug–carrier interactions occur through the Cl—H interaction for the adsorption of *cis*-$[PtCl_2(NH_3)_2]$ and *cis*-$[PtCl(NH_3)_2]^+$, and through Pt—S and Pt—H interactions for *cis*-$[Pt(NH_3)_2]^{2+}$ adsorption. When the new interactions are formed, the functionalised carrier maintains their matrix properties while the molecule is the most affected after adsorption, the major changes are produced in Pt atomic orbitals.

Acknowledgements

Our work was supported by SGCyT UTN, SGCyT UNS, PIP-CONICET 0103 and PICT 1770 and 1186. A. Juan, G. Brizuela and S. Simonetti are members of CONICET. A. Díaz Compañy is a fellow of Comisión de Investigaciones Científicas (CIC) Pcia. Bs. As.

References

[1] C.W. Purnomo and S.Z. Qiao, *Functionalized mesoporous silica utilization for VOCs adsorption*, ASEAN J. Chem. Eng. 7 (2007), p. 43.
[2] N. Garcia, E. Benito, J. Guzman, P. Tiemblo, V. Morales, and R.A. Garcia, *Functionalization of SBA-15 by an acid-catalyzed approach. A surface characterization study*, Micropor. Mesopor. Mater. 106 (2007), p. 129.
[3] Q. Wei, H.Q. Chen, Z.R. Nie, Y.L. Hao, Y.L. Wang, Q.Y. Li, and J.X. Zou, *Preparation and characterization of vinyl-functionalized mesoporous SBA-15 silica by a direct synthesis method*, Mater. Lett. 61 (2007), p. 1469.
[4] Q. Wei, L. Liu, Z.R. Nie, H.Q. Chen, Y.L. Wang, Q.Y. Li, and J.X. Zou, *Functionalization of periodic mesoporous organosilica with ureidopropyl groups by a direct synthesis method*, Micropor. Mesopor. Mater. 101 (2007), p. 381.
[5] G.E. Fryxell, *The synthesis of functional mesoporous materials*, Inorg. Chem. Commun. 9 (2006), p. 1141.
[6] L. Mercier and T.J. Pinnavaia, *Direct synthesis of hybrid organic-inorganic nanoporous silica by a neutral amine assembly route: structure-function control by stoichiometric incorporation of organosiloxane molecules*, Chem. Mater. 12 (2000), p. 188.
[7] M.C. Burleigh, M.A. Markowitz, M.S. Spector, and B.P. Gaber, *Direct synthesis of periodic mesoporous organosilicas, functional incorporation by co-condensation of organosilanes*, J. Phys. Chem. 105 (2001), p. 9935.
[8] Q. Wei, Z.R. Nie, Y.L. Hao, L. Liu, Z.X. Chen, and J.X. Zou, *Effect of synthesis conditions on the mesoscopical order of mesoporous silica SBA-15 functionalized by amino groups*, J. Sol. Gel. Sci. Tech. 39 (2006), p. 103.
[9] J. Kobler, K. Möller, and T. Bein, *Colloidal suspensions of functionalized mesoporous silica nanoparticles*, ACS Nano 2 (2008), p. 791.
[10] G. Wang, A.N. Otuonye, E.A. Blair, K. Denton, Z. Tao, and T. Asefa, *Functionalized mesoporous materials for adsorption and release of different drug molecules: A comparative study*, J. Sol. State Chem. 182 (2009), p. 1649.
[11] Y. Li, B. Yan, and J.-L. Liu, *Luminescent organic-inorganic hybrids of functionalized mesoporous silica SBA-15 by thio-salicylidene schiff base*, Nanoscale Res. Lett. 5 (2010), p. 797.
[12] Yi-Ch. Liu and S.T. Liu, *A recyclable thiol-functionalized mesoporous silica for detection and removal of Cu (II) Ions*, J. Chin. Chem. Soc. 57 (2010), p. 946.
[13] D. Margolese, J.A. Melero, S.C. Christiansen, B. Chmelka, and G.D. Stucky, *Direct syntheses of ordered SBA-15 mesoporous silica containing sulfonic acid groups*, Chem. Mater. 12 (2000), p. 2448.
[14] P.J. O'Dwyer and J.P. Stevenson, *Clinical status of* cis*platin, carboplatin, and other platinum-based antitumor drugs*, in Cis*platin*, B. Lippert, ed., Wiley-VCH, Weinheim, 1999, pp. 31–38.
[15] B. Desoize and C. Madoulet, *Particular aspects of platinum compounds used at present in cancer treatment*, Crit. Rev. Oncol. Hematol. 42 (2002), p. 317.
[16] J. Kai-Chi Lau and D.V. Deubel, *Hydrolysis of the anticancer drug cisplatin: Pitfalls in the interpretation of quantum chemical calculations*, J. Chem. Theory Comput. 2 (2006), p. 103.
[17] Y. Ramos Rodríguez and C. Hernández Castro, *Avances recientes en la determinación analítica del cisplatino y sus productos de hidrólisis*, CENIC Ciencias Químicas 40 (2009), p. 3.
[18] R. Hoffmann and W.N. Lipscom, *Theory of polyhedral molecules. I. Physical factorizations of the secular equation*, J. Chem. Phys. 36 (1962), p. 2179.
[19] R. Hoffmann, *An extended Hueckel theory. I. Hydrocarbons*, J. Chem. Phys. 39 (1963), p. 1397.
[20] M. Whangbo and R. Hoffmann, *The band structure of the tetracyanoplatinate chain*, J. Am. Chem. Soc. 100 (1978), p. 6093.
[21] A. Anderson, *Derivation of the extended Hueckel method with corrections. One electron molecular orbital theory for energy level and structure determinations*, J. Chem. Phys. 62 (1975), p. 1187.
[22] G. Landrum and W. Glassey, *Yet another extended Hückel molecular orbital package (YAeHMOP)*, Cornell University, Ithaca, NY, 2004.
[23] A. Anderson and R. Hoffmann, *Description of diatomic molecules using one electron configuration energies with two-body interactions*, J. Chem. Phys. 60 (1974), p. 4271.

Q6

[24] A. Anderson, *The influence of electrochemical potential on chemistry at electrode surfaces modeled by MO theory*, J. Electroanal. Chem. Interfacial Electrochem. 280 (1990), p. 37.

Q5 [25] J.H. De Boer and J.M. Vleekens, *Proc. K. Ned. Akad. Wet. Ser. B*, Vol. 61, 4th ed. 1958, p. 85.

[26] G.H.W. Milburn and M.R. Truter, *The crystal structures of* cis- *and* trans-*dichlorodiammineplatinum (II)*, J. Chem. Soc. (A) (1966), p. 1609.

Q6

[27] R. Shandles, E.O. Schlemper, and R.K. Murmann, *The crystal and molecular structure of tetraammineplatinum (II) μ-oxo-bis[oxotetracyanorhenium (V)]*, Inorg. Chem. 10 (1971), p. 2785.